Washington University School of Medicine
Digital Commons@Becker

Open Access Publications

2019

Imaging of HER2 with [89Zr]pertuzumab in response to T-DM1 therapy

Adriana V.F. Massicano
University of Alabama, Birmingham

Supum Lee
Yale University

Bryant K. Crenshaw
University of Alabama, Birmingham

Tolulope A. Aweda
University of Alabama, Birmingham

Retta El Sayed
University of Alabama, Birmingham

See next page for additional authors

Follow this and additional works at: https://digitalcommons.wustl.edu/open_access_pubs

Recommended Citation

Massicano, Adriana V.F.; Lee, Supum; Crenshaw, Bryant K.; Aweda, Tolulope A.; El Sayed, Retta; Super, Ian; Bose, Ron; Marquez-Nostra, Bernadette V.; and Lapi, Suzanne E., ,"Imaging of HER2 with [89Zr]pertuzumab in response to T-DM1 therapy." Cancer Biotherapy & Radiopharmaceuticals.34,4. 209-217. (2019).
https://digitalcommons.wustl.edu/open_access_pubs/7742

This Open Access Publication is brought to you for free and open access by Digital Commons@Becker. It has been accepted for inclusion in Open Access Publications by an authorized administrator of Digital Commons@Becker. For more information, please contact engeszer@wustl.edu.

Authors
Adriana V.F. Massicano, Supum Lee, Bryant K. Crenshaw, Tolulope A. Aweda, Retta El Sayed, Ian Super, Ron Bose, Bernadette V. Marquez-Nostra, and Suzanne E. Lapi

This open access publication is available at Digital Commons@Becker: https://digitalcommons.wustl.edu/open_access_pubs/7742

CANCER BIOTHERAPY AND RADIOPHARMACEUTICALS
Volume 34, Number 4, 2019
© Mary Ann Liebert, Inc.
DOI: 10.1089/cbr.2018.2654

Original Articles

Imaging of HER2 with [^{89}Zr]pertuzumab in Response to T-DM1 Therapy

Adriana V.F. Massicano,[1] Supum Lee,[2] Bryant K. Crenshaw,[1] Tolulope A. Aweda,[1] Retta El Sayed,[1] Ian Super,[1] Ron Bose,[3] Bernadette V. Marquez-Nostra,[2] and Suzanne E. Lapi[1]

Abstract

Background: The success of human epidermal growth factor receptor 2 (HER2)-targeted therapy depends on accurate characterization of HER2 expression, but current methods available have several limitations. This study aims to investigate the feasibility of [^{89}Zr]pertuzumab imaging to monitor early response to Ado-trastuzumab emtansine (T-DM1) therapy in mice bearing xenografts of HER2-positive breast cancer (BCa).
Materials and Methods: Pertuzumab was conjugated to DFO-Bz-NCS and labeled with ^{89}Zr. Mice bearing BT-474 tumors were imaged with [^{89}Zr]pertuzumab and [^{18}F]FDG before and after T-DM1 therapy.
Results: Pertuzumab was successfully labeled with ^{89}Zr with a specific activity of 0.740 MBq/μg. Overall [^{18}F]FDG images showed poor delineation of tumors. Using [^{18}F]FDG-PET to measure tumor volume, the volume remained unchanged from 107.6 ± 20.7 mm^3 before treatment to 89.87 ± 66.55 mm^3 after treatment. In contrast, [^{89}Zr]pertuzumab images showed good delineation of HER2-positive tumors, allowing accurate detection of changes in tumor volume (from 243.80 ± 40.91 mm^3 before treatment to 78.4 ± 40.43 mm^3 after treatment).
Conclusion: [^{89}Zr]pertuzumab may be an imaging probe for monitoring the response of HER2-positive BCa patients to T-DM1 therapy.

Keywords: [^{89}Zr]pertuzumab, HER2-positive breast cancer, T-DM1 therapy, molecular imaging, radiolabeled monoclonal antibody

Downloaded by Washington Univ from www.liebertpub.com at 05/13/19. For personal use only.

Introduction

The human epidermal growth factor receptor 2 (HER2) has been extensively studied for several years because of its importance and prevalence in cancer cells. Some cancers, including bladder, lung, gastric, ovarian, prostate, and breast cancer (BCa) may present amplification of the HER2 gene that often leads to the overexpression of the HER2 protein on the cell surface.[1] About 15%–20% of all BCa exhibit HER2 overexpression/amplification and these tumor subtypes are frequently more aggressive with poor prognosis.[2,3] Fortunately, patients with HER2-positive BCa are eligible for HER2-targeted therapy using monoclonal antibodies (mAbs).

The first anti-HER2 mAb approved by Food and Drug Administration (FDA) was trastuzumab (Herceptin®; Genentech, South San Francisco, CA), which binds to the domain IV of HER2, and its use has significantly improved patient survival.[3,4] Several other drugs and mAbs have been developed for use as single agents or in combination with trastuzumab. Pertuzumab (Perjeta®; Genentech), is a humanized mAb that binds to domain II of the extracellular portion of HER2 inhibiting HER2 heterodimerization with other HER family members.[5] It is approved by FDA for use in combination with trastuzumab and docetaxel as a first line therapy for metastatic HER2-positive BCa.[6]

Ado-trastuzumab emtansine (T-DM1, Kadcyla®; Genentech) is a HER2-targeted antibody-drug containing DM1, a derivative of maytansine conjugated to trastuzumab via a stable thioether linker.[7] T-DM1 retains all of trastuzumab's mechanisms of action and adds to it a potent inhibitor of microtubule polymerization (DM1).[8] Clinically, T-DM1 has

[1]Department of Radiology, The University of Alabama at Birmingham, Birmingham, Alabama.
[2]Department of Radiology and Biomedical Imaging, PET Center, Yale University, New Haven, Connecticut.
[3]Division of Oncology, Department of Medicine, Washington University School of Medicine, St. Louis, Missouri.

Address correspondence to: Suzanne E. Lapi; Department of Radiology, The University of Alabama at Birmingham; 1824 6th Avenue South, WTI 310F, Birmingham, AL 35294
E-mail: **lapi@uab.edu**

Downloaded by Washington Univ from www.liebertpub.com at 05/13/19. For personal use only.

been well tolerated by patients with minimal adverse effects and has increased patient survival.[9,10]

Since the success of this type of therapy depends directly on the level of HER2 present on the cell surface, determination of HER2 expression is very important. Currently, there are two types of tests available to measure HER2 status in biopsies: (1) immunohistochemistry (IHC) that detects HER2 overexpression, and (2) fluorescence *in situ* hybridization (FISH) that detects HER2 gene amplification.[11] There is evidence that HER2 expression changes during the course of disease and therapy[12] and for that reason, many protocols encourage repeated biopsies throughout the treatment.[13] However, it has been reported that up to 20% of results using these methods may be inaccurate.[11] Furthermore, since these methods use small sample of biopsied tumors and due to the intra-tumor heterogeneity, these methods may not represent the status of HER2 expression in the whole tumor and/or in the metastatic foci.[1,14]

To develop more specific agents to detect HER2 expression, several groups have labeled mAbs with different radioisotopes for single-photon emission computed tomography (SPECT) and positron emission tomography (PET) imaging. These radiopharmaceuticals used for molecular imaging exhibit an immense advantage because they are HER2-targeted and therefore, are more specific than other imaging techniques. Advantages of targeting HER2 in nuclear medicine are discussed in a recent review.[15] Trastuzumab is the most studied HER2 mAb and in several previous studies, labeled trastuzumab has shown promise as an option to assess HER2 status in patients with HER2-positive BCa.[12,16–21]

In addition to this approach, [^{89}Zr]trastuzumab was used in a recent study to identify patients unlikely to benefit from T-DM1 therapy, illustrating the potential utility of HER2 imaging to improve T-DM1 patient selection.[22]

Nevertheless, during trastuzumab and/or T-DM1 therapy, imaging with radiolabeled trastuzumab may be problematic due to the saturation of epitope IV of HER2 receptors. Several studies show pertuzumab does not compete with trastuzumab *in vitro* and *in vivo*,[23–25] since they bind to a different epitope of HER2.[5] Interestingly, one recent study illustrated the presence of trastuzumab enhanced radiolabeled pertuzumab uptake in HER2-positive tumors.[23] Therefore, using imaging agents based on pertuzumab while treating with trastuzumab or T-DM1 may allow a more sensitive detection of HER2 without binding competition.[23]

This study aimed to evaluate the utility of [^{89}Zr]pertuzumab to monitor early response to T-DM1 therapy in xenograft mice bearing HER2-positive BCa.

Materials and Methods

Antibodies and reagents

The production of ^{89}Zr-oxalate was carried out in house (University of Alabama at Birmingham, Cyclotron Facility) using ^{89}Y sputtered solid targets as described previously.[26] Pertuzumab (Perjeta) and Ado-trastuzumab emtasine (Kadcyla) were purchased from Genentech. Anti-HER2 (Neu C-18; sc-284), anti-β actin (sc-47778 HRP), and goat antirabbit IgG-HRP (sc-2054) antibodies for western blotting were purchased from Santa Cruz Biotechnology (Dallas, TX). Desferrioxamine-p-benzyl-isothiocyanate (DFO-Bz-NCS) was purchased from Macrocyclics (Dallas, TX). Dimethyl sulfoxide (DMSO) and sodium carbonate were purchased from Sigma-Aldrich (St. Louis, MO). HEPES was purchased from ACROS Organic (Fair Lawn, NJ). All other chemicals were purchased from Fisher Scientific (Hampton, NH) unless stated otherwise.

Cell culture

The BT-474 (HER2-positive) cell line was purchased from American Type Culture Collection (ATCC) and cultivated in Dulbecco's Modified Eagle Medium (DMEM) containing 10% fetal bovine serum (FBS) and 10 mg/mL gentamycin in a humidified incubator with 5% CO_2 at 37°C. BT-474 cells were supplemented with 0.01 mg/mL of human insulin (Sigma-Aldrich, St. Louis, MO). JIMT-1 (HER2-positive) cell was purchased from AddexBio (San Diego, CA) and cultivated in Iscove's Modified Dulbecco's Medium (IMDM) with 10% FBS and gentamycin (10 mg/ML) at the same conditions cited above. All other reagents for cell culture were purchased from Gibco® Life Technologies (Grand Island, NY).

Preparation of [^{89}Zr]pertuzumab

Conjugation of DFO-Bz-NCS to pertuzumab and radiolabeling with ^{89}Zr-oxalate were performed following previous methods.[23,27] Briefly, 8, 10, 16, and 20-fold molar excess of DFO-Bz-NCS dissolved in DMSO were incubated with pertuzumab in 0.1 M sodium carbonate buffer (pH 9) at 37°C for 1 h. After the conjugation, the DFO-pertuzumab conjugate was purified and buffer exchanged into 1 M HEPES buffer pH 7.1–7.3 via Zeba spin desalting columns (40 kDa Molecular Weight Cut-Off; Thermo Scientific, Rockford, IL). The final concentration of protein was quantified using a bicinchoninic acid (BCA) assay (Thermo Scientific, Rockford, IL). The purified DFO-pertuzumab was labeled with neutralized ^{89}Zr-oxalate using an activity of 0.148, 0.296, 0.370, and 0.710 MBq per μg mAb in a final volume of 100 μL at 37°C for 1 h.

The radiochemical yield (RCY) was determined by instant thin-layer chromatography (iTLC) using 50 mM DTPA as the developing solution or by size exclusion high performance liquid chromatography (SE-HPLC) using a size-exclusion column (BioSep SECs-3000, 300 × 7.8 mm, 5 μm, Phenomenex, CA) and 50 mM sodium phosphate, 150 mM sodium chloride, 0.1%Tween-20 buffer as mobile phase, at a flow rate of 1 mL/min. [^{89}Zr]pertuzumab with RCYs ≥95% chromatography was used for *in vitro* and *in vivo* studies without further purification. When the yield was lower than 95%, [^{89}Zr]pertuzumab was purified using Zeba spin desalting columns to achieve radiochemical purity (RCP) ≥95%.

Immunoreactivity

The immunoreactivity of conjugates was determined using the Lindmo[28] assay in BT-474 cells. Briefly, cells were harvested with trypsin and diluted in 1.5 mL microcentrifuge tubes at a concentration ranging from 0.250 to 2.5×10^6 BT-474 cells in phosphate buffered saline (PBS). An aliquot of [^{89}Zr]pertuzumab was diluted in 1% bovine serum albumin

Downloaded by Washington Univ from www.liebertpub.com at 05/13/19. For personal use only.

in PBS (1–2 μCi in 10 mL) and added to the BT-474 cells. The cells were incubated for 1 h at room temperature with gentle rocking. Afterward, the microcentrifuge tubes were centrifuged and the pelleted cells obtained were washed three times with cold PBS. The data were plotted as total activity added to the cells/total activity bound to the cells (Y axis) *versus* the cell concentration (mL/million) (X axis). Afterward, the graph was fit by a linear regression using Microsoft Excel 2010 software. The immunoreactivity was calculated by (1/Y intercept) multiplied by 100.

Stability study in vitro

[^{89}Zr]pertuzumab was diluted in NaCl 0.9% (0.1 MBq/μL), incubated at either 4°C ± 2°C or room temperature for 48 h. At specific time points (1, 4, 24, and 48 h), aliquots of 1 μL were spotted on ITLC plates and the RCY evaluated as described previously. The stability was also evaluated in human and mouse serum *in vitro* by SE-HPLC. [^{89}Zr]pertuzumab was diluted in human or mouse serum (Fisher Scientific, MA) to a radioactivity concentration of 37 MBq/mL. A control consisted of [^{89}Zr]pertuzumab diluted in PBS. The samples were incubated at 37°C for 7 d. Aliquots of 30 μL were analyzed in duplicate by SE-HPLC daily using protocol described above. The radioactive peaks were analyzed using a Sodium Iodide (NaI) detector (Lab Logic, FL) coupled with an Agilent HPLC (model 1260 Infinity; Agilent, CA), equipped with Laura software (version 4.5; Lab Logic).

Specific cell binding in vitro

The specific binding of [^{89}Zr]pertuzumab was assessed in BT-474 and JIMT-1 cells *in vitro*. Cells (1×10^6) were incubated with [^{89}Zr]pertuzumab (5 nM in IMDM or DMEM 1% FBS) alone (total binding) or in presence of cold pertuzumab (5 μM in IMDM or DMEM 1% FBS) (competitive binding) for 1.5 h at room temperature with gentle rocking. The cells were washed with PBS and assayed in a gamma counter. The percentage of [^{89}Zr]pertuzumab bound to the cells in presence or absence of competitor was calculated.

Western blotting

BT-474 and JIMT-1 cells were lysed with RIPA buffer (Alfa Aesar, MA) and the protein concentration in the extracted lysates was measured by BCA assay. Proteins (20 μg) were loaded onto Any kD Mini-PROTEAN TG precast gels (Biorad, Hercules, CA) in Tris/Glycin/SDS buffer for electrophoresis. For western blotting, the proteins in the gel separated by electrophoresis were transferred onto PVDF membranes (Biorad). The membranes were blocked with 3% nonfat dry milk (NFDM) in PBST for 1 h at room temperature and incubated with anti-HER2 primary antibody (C-18, 1 μg/mL in 3% NFDM) overnight at 4°C. The membranes were then washed and incubated with goat antirabbit HRP-conjugated antibody (50 ng/mL in 3% NFDM) and anti-β actin (100 ng/mL in 3% NFDM) for 1 h at room temperature. After extensive washing, the membranes were incubated with a chemiluminescent western blotting detection reagent (ECL Select; GE Healthcare, Chicago, IL) according to manufacturer's instructions and measured using a ChemiDoc XRS+ imager (Biorad). The HER2 bands were normalized by the amount of protein loaded (β-actin band) using ImageJ software (National Institutes of Health, Bethesda, MD).

Animal studies

Tumor model. All animal experiments were performed in accordance with guidelines of the Institutional Animal Care and Use Committee (IACUC) at the University of Alabama at Birmingham under an approved animal protocol. *In vivo* PET imaging studies were conducted in 5-week-old athymic nu/nu female mice (Charles River Laboratories, Wilmington, MA). A schema of *in vivo* tumor model and therapy protocol used in this work is shown in Figure 1. Mice were subcutaneously implanted with 60-d release pellets containing 0.72 mg of 17β-estradiol (Innovative Research of America, Sarasota, FL) on day −52. One week after the pellet implantation (day −45), mice were subcutaneously inoculated on the left shoulder with 1×10^7 cells/mL of BT-474 cells suspended in 100 μL PBS. Tumors were allowed to grow for 5 weeks.

Evaluation of tumor size changes after T-DM1 treatment in BT-474 HER2-positive xenografted mice. Mice were divided into 2 groups of 4 mice (control and treatment). On day −7 (Fig. 1), mice were injected via tail-vein with 7.4 MBq (200 μCi) of 2-deoxy-2-[^{18}F]fluoro-D-glucose ([^{18}F]FDG; PETNET Solutions, Birmingham, AL) and static PET baseline images were acquired for 20 min, 1 h postinjection (p.i) using a Flex Triumph small animal PET/CT (TriFoil Imaging, Chatsworth, CA). On day −6, the same mice were injected via tail-vein with 3.7 MBq (100 μCi) of [^{89}Zr]pertuzumab (specific activity 592 MBq/mg) diluted in saline and static PET baseline images were acquired as described above at 5 d p.i. On day 0 mice belonging to the treatment group received 15 mg/kg of T-DM1 diluted in 100 μL of saline via tail-vein while mice belonging to the control group received 100 μL of saline via tail-vein.

Two weeks after the T-DM1 administration, (on day +14) the imaging protocols using [^{18}F]FDG and [^{89}Zr]pertuzumab were repeated. The images were reconstructed using a

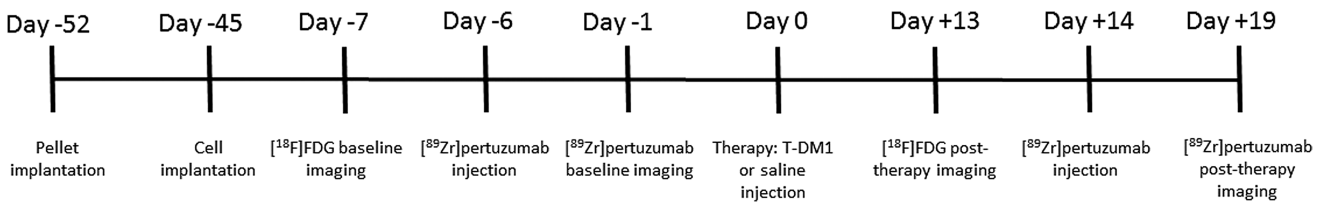

FIG. 1. *In vivo* tumor model development and therapy protocol schema.

MLEM three-dimensional protocol and analyzed by Inveon Research Workplace software (Siemens, Knoxville, TN). The tumor volumes were calculated by region of interest (ROI) drawn on the PET/CT images before and after T-DM1 therapy. The standard uptake value (SUV) was calculated by the following formula:

$$SUV = \frac{r}{a' \times w}$$

Where r is the radioactivity concentration [kBq/mL] within a ROI, a′ is the decay-corrected amount of injected radiopharmaceutical [kBq], and w is the mouse weight [g].

The changes in tumor size were evaluated by caliper weekly and by PET/CT imaging as described above.

HER2 quantification in tumors. The tumors were excised following the final imaging session and flash frozen in liquid nitrogen. Tissues were pulverized using a cell crusher and

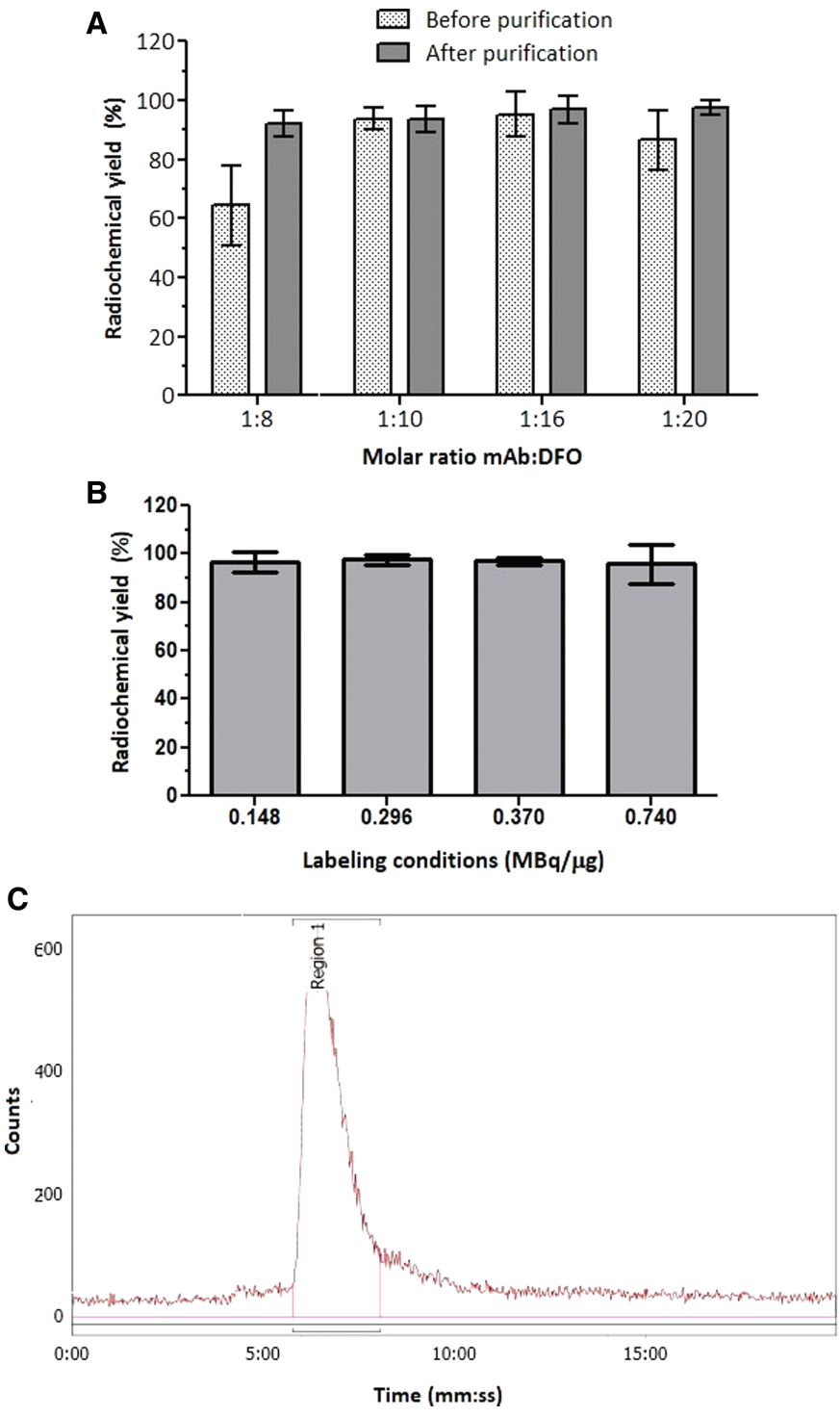

FIG. 2. RCY of pertuzumab conjugated to DFO at different molar ratios and labeled with ^{89}Zr at 4 μCi/μg **(A)**; RCY of pertuzumab conjugated to DFO at molar ratio 1:16 and labeled with ^{89}Zr at different ratios **(B)**; Radiochromatogram of [^{89}Zr]pertuzumab **(C)**. RCY, radiochemical yield. Color images are available online.

Downloaded by Washington Univ from www.liebertpub.com at 05/13/19. For personal use only.

proteins were extracted using RIPA buffer. HER2 quantification was conducted using a Quantikine® ELISA kit (R&D Systems, MN) following supplier instructions. Concentrations of HER2 were normalized to total protein using BCA assay.

Statistical analysis

Statistical analysis was performed using Student's *t*-test ($p < 0.05$) for single comparison and one-way or two-way analysis of variance for multiple comparison followed by Bonferroni post-test. All analyses were performed on GraphPad Prism V5 (GraphPad Software, Inc., La Jolla, CA).

Results

Preparation and characterization of [^{89}Zr]pertuzumab

Pertuzumab was conjugated to DFO-Bz-NCS by combining 8, 10, 16, or 20 moles of chelator to 1 mole of mAb at pH 9 for 1 h at 37°C, followed by prompt purification. The conjugated antibody was labeled with ^{89}Zr (0.148 MBq/μg). The RCY achieved for the molar ratio 1:8 were significantly lower ($p < 0.05$) compared with molar ratios 1:10 and 1:16. For molar ratios 1:10 and 1:16 the RCY were higher than 90% without any further purification. When a purification step was added, all molar ratios presented RCP greater than 92%; the molar ratios 1:16 and 1:20 showed RCP superior to 95% (Fig. 2A).

The mAb conjugated at molar ratio 1:16 was labeled with ^{89}Zr at different activity concentrations and showed RCY greater than 95% for all conditions studied with no additional purification needed (Fig. 2B). This molar ratio allowed a specific activity of 0.740 MBq/μg with minimum formation of aggregates after labeling, as showed by SE-HPLC (Fig. 2C).

Stability in NaCl 0.9% and human serum

The radiochemical stability of [^{89}Zr]pertuzumab in 0.9% NaCl was used to inform the expiration time of [^{89}Zr]pertuzumab to plan further *in vitro* and *in vivo* experiments. Four different lots of labeled antibody were evaluated by iTLC up to 48 h at two different storage temperature (room temperature and at 2°C–8°C). All lots presented RCP of 99.94% ± 0.06% at the time of preparation. After 24 h, the labeled antibody presented a RCP of 96.08% ± 1.89% when incubated at 2°C–8°C and 93.63% ± 1.67%, $n = 4$, ($p = 0.368$) when incubated at room temperature (Fig. 3A). When the RCP at 24 h was compared to the initial RCP, the incubation at 4°C ± 2°C showed no significant difference ($p = 0.088$), while the incubation at room temperature showed significantly lower RCP ($p = 0.009$), indicating this storage condition is not ideal for this compound. After 48 h at room temperature, the RCP decreased more than 10% from the initial value (87.77% ± 3.20%) while storage at 2°C–8°C resulted in better preservation of the RCP after 48 h of incubation (91.98% ± 3.56%).

[^{89}Zr]pertuzumab was incubated in PBS, human and mouse serum at 37°C up to 7 d and stability was evaluated by SE-HPLC (Fig. 3B). For all three conditions, the RCP corresponds to [^{89}Zr]pertuzumab monomer, which decreased by 12% in 24 h.

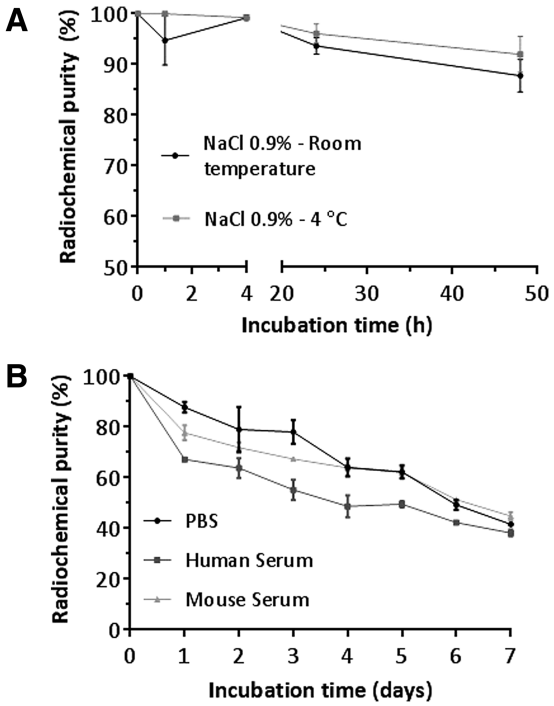

FIG. 3. Stability of [^{89}Zr]pertuzumab in NaCl 0.9% at room temperature and 4°C **(A)**. Stability of [^{89}Zr]pertuzumab in human serum, mouse serum, and PBS at 37°C **(B)**. PBS, phosphate buffered saline.

For incubation in mouse and human serum, it was observed that the RCP decrease was mostly due to the formation of aggregates or transchelation of ^{89}Zr to serum proteins. However, after day 5, free ^{89}Zr was observed in the chromatograms for both conditions. For [^{89}Zr]pertuzumab incubated in PBS the main impurity observed was free ^{89}Zr with minimal formation of aggregates.

Cell binding studies in vitro *and western blotting*

HER2-positive BT-474 cells were used to determine [^{89}Zr]pertuzumab immunoreactivity by Lindmo assay. The immunoreactivity fraction was calculated to be 79.4% ± 6.1%; 74% ± 11.8%; 75.1% ± 1.0%; and 67.2% ± 2.4% for molar ratios 1:8, 1:10, 1:16, and 1:20 respectively. At molar ratio 1:20, the immunoreactivity decreased more than 10% compared to the labeling at a molar ratio 1:8, however, this difference was not significant ($p = 0.1191$).

The specificity of [^{89}Zr]pertuzumab binding to HER2 cells was investigated in BT-474 and JIMT-1 cells (Fig. 4A). Significantly higher binding was observed in BT-474 (36.46% ± 0.05% of total radioactivity added) compared to JIMT-1 (7.30% ± 0.02% of total radioactivity added) ($p < 0.01$). For both cells, competitive binding studies showed decreased uptake of [^{89}Zr]pertuzumab in the presence of non-labeled antibody (0.18% ± 0.09% and 0.24% ± 0.05% of total radioactivity added for BT-474 and JIMT-1 cells respectively), demonstrating that the uptake of [^{89}Zr]pertuzumab was HER2-specific.

Downloaded by Washington Univ from www.liebertpub.com at 05/13/19. For personal use only.

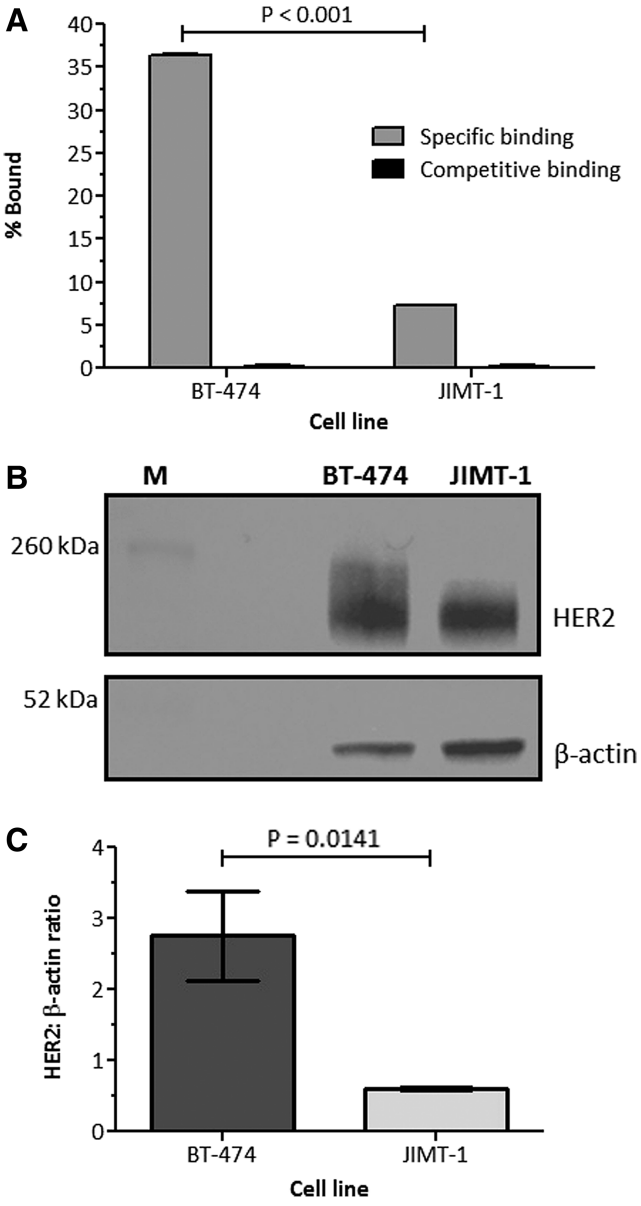

FIG. 4. Uptake of [^{89}Zr]pertuzumab in BT-474 and JIMT-1 cells **(A)**. Western blot of BT-474 and JIMT-1. Anti-HER2 antibody (C-18) was used to characterize the HER2 expression, and expression of β-actin was used as the loading control **(B)**. HER2:β-actin ratio for BT-474 and JIMT-1 cells **(C)**. HER2, human epidermal growth factor receptor 2.

HER2 expression in BT-474 and JIMT-1 was evaluated by western blotting assay. A strong band with molecular weight of 185 kDA, corresponding to HER2 protein, was observed in both cell lines; however, the band in BT-474 cells was stronger than JIMT-1 (Fig. 4B). After normalization to total protein loaded (β-actin band), the HER2:β-actin ratio was significantly higher for BT-474 cells than for JIMT-1 cells ($p = 0.0141$; Fig. 4C) and this result corroborates with the cell binding assay results. Due to the higher HER2 expression found in BT-474 cells, this cell line was used for all following experiments.

Development of mice tumor model

Estrogen pellets are commonly used to stimulate tumor growth of BT-474 cells in athymic nude mice. Using this technique, we observed a tumor take rate of 100% after 5 weeks of cell implantation. However, the tumors were varied in size ($250.35 \pm 167.82\,mm^3$). For this reason, mice were divided in two groups of similar tumor sizes.

Evaluation of tumor size changes after T-DM1 treatment in BT-474 HER2-positive xenograft mice

Tumors measured by caliper 2 weeks post T-DM1 therapy showed the treated tumors decreased by 48% in volume whereas the tumor volume in the control group increased by 219% (Fig. 5A).

The variance in tumor size as a consequence of T-DM1 therapy was also evaluated by PET/CT imaging. Baseline and post T-DM1 therapy images were acquired using [^{18}F]FDG and [^{89}Zr]pertuzumab produced in the optimized conditions (molar ratio DFO:mAb of 1:16; labeling condition of 0.740 MBq/μg).

The [^{18}F]FDG images showed nonspecific uptake in heart and brown fat with relatively little tumor uptake (Fig. 6A, C). In contrast, [^{89}Zr]pertuzumab images showed intense tumor

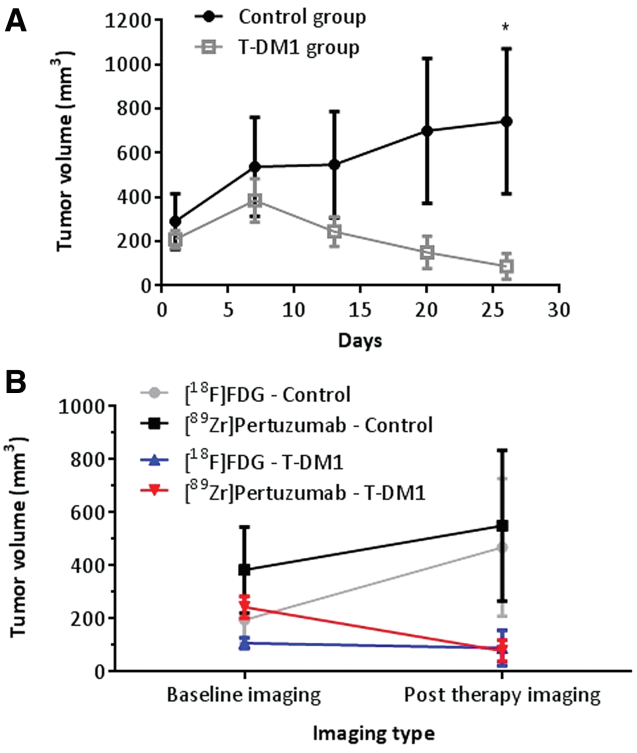

FIG. 5. Effect of T-DM1 therapy in HER2-positive BCa BT-474 xenograft. Athymic nude mice bearing BT-474 tumors were treated (4 mice per group) with saline (control group) or T-DM1 (15 mg/kg, single administration, i.v.). Tumor volume was measured weekly by caliper **(A)** and by using ROI from PET/CT images before and after therapy using [^{18}F]FDG and [^{89}Zr]pertuzumab as a radiopharmaceutical **(B)**. BCa, breast cancer; CT, computed tomography; PET, positron emission tomography; ROI, region of interest; T-DM1, Ado-trastuzumab emtansine. Color images are available online.

Downloaded by Washington Univ from www.liebertpub.com at 05/13/19. For personal use only.

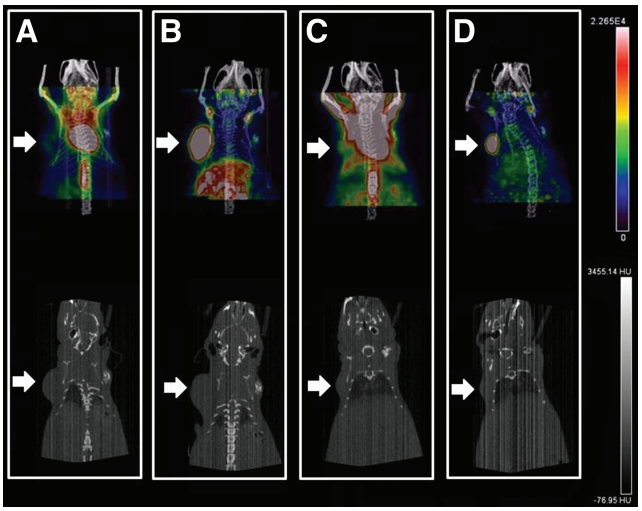

FIG. 6. Posterior half body PET/CT images of Nu/Nu mice implanted with BT-474 human BCa xenografts (*white arrows*). Baseline imaging acquired before therapy with T-DM1 using [18F]FDG **(A)** and [89Zr]pertuzumab **(B)** and after therapy using [18F]FDG **(C)** and [89Zr]pertuzumab **(D)**. Color images are available online.

uptake with only modest uptake in normal organs. Furthermore, the images with [89Zr]pertuzumab showed good tumor delineation that led to clear visualization of changes in tumor size after T-DM1 therapy (Fig. 6B, D).

Attempts to delineate the tumor using only CT images (Fig. 6 bottom row), were unsuccessful as after T-DM1 therapy the tumors became too small to identify via CT in the treated group. Although CT is used clinically, it may not be ideal to measure regression of tumors in patients with high specificity. [89Zr]pertuzumab PET/CT images showed significantly better tumor delineation than [18F]FDG (Fig. 5B). [89Zr]pertuzumab PET/CT images allowed for detection of changes in tumor volume in the T-DM1 group (from $243.8 \pm 40.91\,mm^3$ to $78.40 \pm 40.43\,mm^3$; $p = 0.0282$), which also corresponded to caliper measurements, however, [18F]FDG poorly detected tumor volume changes in the T-DM1 group ($107.60 \pm 20.72\,mm^3$ to $80.87 \pm 66.55\,mm^3$; $p = 0.7824$) (Fig. 5B).

Table 1. Standard Uptake Value Mean Calculated Before (Baseline Imaging) and After T-DM1 Therapy Using [18F]FDG and [89Zr]pertuzumab Positron Emission Tomography/Computed Tomography

Radiopharmaceutical and group	*SUV mean baseline imaging*	*SUV mean post therapy imaging*
[18F]FDG—control group	3.8 ± 0.9	4.7 ± 3.1
[89Zr]pertuzumab—control group	40.6 ± 7.5	43.2 ± 8.3
[18F]FDG—T-DM1 group	4.0 ± 1.9	3.5 ± 3.4
[89Zr]pertuzumab—T-DM1 group	41.9 ± 2.0	47.5 ± 15.9

SUV, standard uptake value; T-DM1, Ado-trastuzumab emtansine.

The mean SUV for both imaging time points, showed that [89Zr]pertuzumab had a significantly higher SUV before and after therapy when compared with [18F]FDG ($p < 0.0001$; Table 1). However, there were no significant changes in the SUV before and after therapy for both radiopharmaceuticals ($p > 0.05$).

HER2 quantification in the tumors indicated there was no difference ($p = 0.1196$) between HER2 concentration in the control group (0.213 ± 0.217 pg/mL of HER2 per tumor) and the group treated with T-DM1 (0.016 ± 0.009 pg/mL of HER2 per tumor). This result is in agreement with the lack of change in [89Zr]pertuzumab tumor uptake before and after treatment. Thus, T-DM1 treatment did not impact HER2 expression in our model.

Discussion

HER2-positive BCa represents approximately 20% of all BCa and HER2 expression is associated with poor prognosis and more aggressive cancer subtypes [3]. Patients who have HER2-positive cancers can benefit from targeted therapy using targeted mAbs. As the success of this therapy relies directly on levels of HER2 present in the tumor, an accurate quantification of HER2 expression is crucial. In this scenario, molecular imaging can provide a better tool for patient stratification, and monitoring during the course of therapy.

In this article we describe the use of [89Zr]pertuzumab as a radiopharmaceutical for monitoring response to T-DM1 therapy in mice bearing BT-474 tumors. Our data demonstrate high tumor uptake of [89Zr]pertuzumab in HER2-positive BCa tumors with minimal nonspecific on nontarget organs. Also, our data confirm that [18F]FDG is not suitable for monitoring pharmacological response of the tumor to T-DM1 in this model. This result is in agreement with Janjigian et al. that showed [89Zr]trastuzumab was more specific for imaging of HER2-positive gastric cancer than [18F]FDG.[20]

Pertuzumab was successfully conjugated to DFO using a molar ratio 1:16 that resulted in acceptable conservation of immunoreactivity ($75.1\% \pm 1.0\%$). In addition, by using this molar ratio conditions, we achieved a specific activity of 740 MBq/mg with RCY greater than 95% with no additional purification or formation of aggregates after the labeling, as shown by SE-HPLC.

The RCP of [89Zr]pertuzumab decreased by less than 4% (from $99.94\% \pm 0.06\%$ to $96.08\% \pm 1.89\%$) when it was stored in 0.9% NaCl for 24 h at 2°C–8°C indicating the expiration time can be set for 24 h after labeling when stored under this condition. The labeled antibody showed less stability in human serum than in mouse serum (Fig. 3B). The main impurity formed during the incubation in mouse and human serum was aggregates or transchelation of 89Zr to serum proteins, which might be explained by enzymatic degradation of the antibody in presence of serum.

Our data showed that measurement of the tumor volume was similar with caliper or [89Zr]pertuzumab PET-CT images (Fig. 5A, B) and both methods could detect the significant tumor volume changes after T-DM1 therapy. However, the tumor volume remained unchanged as assessed by [18F]FDG PET/CT. [18F]FDG images showed nonspecific uptake in heart and brown fat with relatively

Downloaded by Washington Univ from www.liebertpub.com at 05/13/19. For personal use only.

little tumor uptake. In contrast, [^{89}Zr]pertuzumab images showed more specificity *in vivo* with good tumor delineation, which led to clear visualization of changes in tumors size after T-DM1 therapy.

No significant changes in the SUV values were observed before and after therapy for both radiopharmaceuticals ($p > 0.05$). This result suggests that even though the therapy was effective, as evidenced by tumor size regression, it did not affect tumor metabolism and/or HER2 expression.

Computed tomography is often used to investigate tumor mass in patients. Although it is possible to detect the tumor volume changes in our model using only CT images (Fig. 6), the tumor margins were not clearly visible. This characteristic hampered accurate assessment of tumor volumes changes via CT especially among the treated group.

Another important finding from this study is that T-DM1 did not downregulate HER2 expression and even though the tumor decreased in size, HER2 concentration was similar in both groups as measured by ELISA. In this particular model, continuing the therapy with T-DM1 or another HER2-targeted therapy would be possible.

Although promising, our study has limitations. First, the sample size of each group was small. Therefore, any findings from this study may be limited by the small sample size. However, it is known that the BT-474 animal model is sensitive to T-DM1, so the response to the treatment was expected.[29–31] Second, we used a cell line with high expression of HER2. Further studies using another cell line with different HER2 expression are warranted to evaluate whether [^{89}Zr]pertuzumab would be able to identify changes in the tumor volume in models with variable HER2 expression.

Our study shows [^{89}Zr]pertuzumab can be used to monitor the efficacy of T-DM1 therapy even after a single therapeutic dose and may aid in determining whether treatment is effective in patients undergoing T-DM1 or trastuzumab therapy to help guide physicians toward tailored treatment for each patient. This hypothesis is reinforced by a recent study published by Ulaner et al. This first-in-human study evaluated the dosimetry and tissues biodistribution of [^{89}Zr]pertuzumab in patients with metastatic BCa HER2-positive. Even though, all 6 patients enrolled had metastasis previously treated with systemic therapy and HER2-targeted therapy, the authors conclude that these therapies did not interfere in the HER2-targeted imaging with [^{89}Zr]pertuzumab.[32]

Other potential applications of [^{89}Zr]pertuzumab are the selection of patients for therapy with trastuzumab and T-DM1 based on their HER2 expression levels and the assessment of HER2 heterogeneity. In these settings, [^{89}Zr]pertuzumab might have an advantage over the methods currently used to measure HER2 status using biopsies (IHC and FISH).

Conclusions

[^{89}Zr]pertuzumab showed high uptake in HER2-positive tumor with high selectivity that led to clear visualization of changes in tumor size after T-DM1 therapy. This radiopharmaceutical showed potential for noninvasive detection of initial response of HER2-positive BCa undergoing T-DM1 therapy *in vivo.*

Acknowledgments

This study was supported by UAB Department of Radiology. The authors would like to thank the members of the Lapi lab, the UAB Cyclotron Facility for production of ^{89}Zr and Emily Brown for additional experimental assistance. The UAB small animal imaging facility is supported through the UAB Comprehensive Cancer Center P30CA013148.

Authors' Contributions

A.V.F.M: conception (constructing the idea for research and the article); design (planning methodology to reach the conclusion); data collection (taking responsibility in execution of the experiments); analysis and interpretation (interpretation and presentation of the results); data processing (taking responsibility in data management and reporting); literature review; writer (taking responsibility in the construction of the article). B.K.C.: data collection (execution of the experiments); review (reviewing the article grammar). S.L., T.A.A., R.E.S., and I.S.: data collection (execution of the experiments); critical review (reviewing the article before submission). R.B. and S.E.L.: conception (constructing the idea for research); critical review (reviewing the article before submission). B.V.M.-N.: conception (constructing the idea for research); design (planning methodology to reach the conclusion); data collection (taking responsibility in execution of the experiments); analysis and interpretation (interpretation and presentation of the results); critical review (reviewing the article before submission).

Disclosure Statement

There are no existing financial conflicts.

References

1. Gebhart G, Flamen P, De Vries EG, et al. Imaging diagnostic and therapeutic targets: Human epidermal growth factor receptor 2. J Nucl Med 2016;57:81s.
2. Slamon DJ, Clark GM, Wong SG, et al. Human breast cancer: Correlation of relapse and survival with amplification of the HER-2/neu oncogene. Science 1987;235:177.
3. Asif HM, Sultana S, Ahmed S, et al. HER-2 positive breast cancer—A mini-review. Asian Pac J Cancer Prev 2016;17:1609–1615.
4. Romond EH, Perez EA, Bryant J, et al. Trastuzumab plus adjuvant chemotherapy for operable HER2-positive breast cancer. N Engl J Med 2005;353:1673.
5. Scheuer W, Friess T, Burtscher H, et al. Strongly enhanced antitumor activity of trastuzumab and pertuzumab combination treatment on HER2-positive human xenograft tumor models. Cancer Res 2009;69:9330.
6. Baselga J, Cortes J, Kim SB, et al. Pertuzumab plus trastuzumab plus docetaxel for metastatic breast cancer. N Engl J Med 2012;366:109.
7. Lewis Phillips GD, Li G, Dugger DL, et al. Targeting HER2-positive breast cancer with trastuzumab-DM1, an antibody-cytotoxic drug conjugate. Cancer Res 2008;68:9280.
8. Junttila TT, Li G, Parsons K, et al. Trastuzumab-DM1 (T-DM1) retains all the mechanisms of action of trastuzumab and efficiently inhibits growth of lapatinib insensitive breast cancer. Breast Cancer Res Treat 2011;128:347.

Downloaded by Washington Univ from www.liebertpub.com at 05/13/19. For personal use only.

9. Krop I, Winer EP. Trastuzumab emtansine: A novel antibody–drug conjugate for HER2-positive breast cancer. Clin Cancer Res 2014;20:15.
10. Vici P, Pizzuti L, Michelotti A, et al. A retrospective multicentric observational study of trastuzumab emtansine in HER2 positive metastatic breast cancer: A real-world experience. Oncotarget 2017;8:56921.
11. Phillips KA, Marshall DA, Haas JS, et al. Clinical practice patterns and cost-effectiveness of HER2 testing strategies in breast cancer patients. Cancer 2009;115:5166.
12. Laforest R, Lapi SE, Oyama R, et al. [^{89}Zr]Trastuzumab: Evaluation of radiation dosimetry, safety, and optimal imaging parameters in women with HER2-positive breast cancer. Mol Imaging Biol 2016;18:952.
13. Li L, Wu Y, Wang Z, et al. SPECT/CT imaging of the novel HER2-targeted peptide probe ^{99m}Tc-HYNIC-H6F in breast cancer mouse models. J Nucl Med 2017;58:821.
14. Yamaguchi H, Tsuchimochi M, Hayama K, et al. Dual-labeled near-infrared/^{99m}Tc imaging probes using PAMAM-coated silica nanoparticles for the imaging of HER2-expressing cancer cells. Int J Mol Sci 2016;17:pii: E1086.
15. Massicano AVF, Marquez-Nostra BV, Lapi SE. Targeting HER2 in nuclear medicine for imaging and therapy. Mol Imaging 2018;17:1.
16. Chang AJ, Desilva R, Jain S, et al. ^{89}Zr-radiolabeled trastuzumab imaging in orthotopic and metastatic breast tumors. Pharmaceuticals (Basel) 2012;5:79.
17. Dijkers EC, Kosterink JG, Rademaker AP, et al. Development and characterization of clinical-grade ^{89}Zr-trastuzumab for HER2/neu immunoPET imaging. J Nucl Med 2009;50:974.
18. Dijkers EC, Oude Munnink TH, Kosterink JG, et al. Biodistribution of ^{89}Zr-trastuzumab and PET imaging of HER2-positive lesions in patients with metastatic breast cancer. Clin Pharmacol Ther 2010;87:586.
19. Gaykema SB, Brouwers AH, Hovenga S, et al. Zirconium-89-trastuzumab positron emission tomography as a tool to solve a clinical dilemma in a patient with breast cancer. J Clin Oncol 2012;30:e74.
20. Janjigian YY, Viola-Villegas N, Holland JP, et al. Monitoring afatinib treatment in HER2-positive gastric cancer with ^{18}F-FDG and ^{89}Zr-trastuzumab PET. J Nucl Med 2013;54:936.
21. Ulaner GA, Hyman DM, Ross DS, et al. Detection of HER2-positive metastases in patients with HER2-negative primary breast cancer using ^{89}Zr-trastuzumab PET/CT. J Nucl Med 2016;57:1523.
22. Gebhart G, Lamberts LE, Wimana Z, et al. Molecular imaging as a tool to investigate heterogeneity of advanced HER2-positive breast cancer and to predict patient outcome under trastuzumab emtansine (T-DM1): The ZEPHIR trial. Ann Oncol 2016;27:619.
23. Marquez BV, Ikotun OF, Zheleznyak A, et al. Evaluation of ^{89}Zr-pertuzumab in Breast cancer xenografts. Mol Pharm 2014;11:3988.
24. Cortes J, Swain SM, Kudaba I, et al. Absence of pharmacokinetic drug-drug interaction of pertuzumab with trastuzumab and docetaxel. Anticancer Drugs 2013;24:1084.
25. Fuentes G, Scaltriti M, Baselga J, et al. Synergy between trastuzumab and pertuzumab for human epidermal growth factor 2 (Her2) from colocalization: An in silico based mechanism. Breast Cancer Res 2011;13:R54.
26. Queern SL, Aweda TA, Massicano AVF, et al. Production of Zr-89 using sputtered yttrium coin targets. Nucl Med Biol 2017;50:11.
27. Vosjan MJ, Perk LR, Visser GW, et al. Conjugation and radiolabeling of monoclonal antibodies with zirconium-89 for PET imaging using the bifunctional chelate p-isothiocyanatobenzyl-desferrioxamine. Nat Protoc 2010;5:739.
28. Lindmo T, Boven E, Cuttitta F, et al. Determination of the immunoreactive fraction of radiolabeled monoclonal antibodies by linear extrapolation to binding at infinite antigen excess. J Immunol Methods 1984;72:77.
29. Al-Saden N, Cai Z, Reilly RM. Tumor uptake and tumor/blood ratios for ^{89}Zr-DFO-trastuzumab-DM1 on microPET/CT images in NOD/SCID mice with human breast cancer xenografts are directly correlated with HER2 expression and response to trastuzumab-DM1. Nucl Med Biol 2018;67:43.
30. Barok M, Tanner M, Koninki K, et al. Trastuzumab-DM1 causes tumour growth inhibition by mitotic catastrophe in trastuzumab-resistant breast cancer cells in vivo. Breast Cancer Res 2011;13:R46.
31. Barok M, Tanner M, Koninki K, et al. Trastuzumab-DM1 is highly effective in preclinical models of HER2-positive gastric cancer. Cancer Lett 2011;306:171.
32. Ulaner GA, Lyashchenko SK, Riedl C, et al. First-in-human human epidermal growth factor receptor 2-targeted imaging using ^{89}Zr-pertuzumab PET/CT: Dosimetry and clinical application in patients with breast cancer. J Nucl Med 2018;59:900.

Downloaded by Washington Univ from www.liebertpub.com at 05/13/19. For personal use only.